ELSEVIER

Physics of the Earth and Planetary Interiors 114 (1999) 25–38

PHYSICS OF THE EARTH AND PLANETARY INTERIORS

Multi-component wavefield simulation in viscous extensively dilatancy anisotropic media

Zhongjie Zhang [a,*], Guangjie Wang [a], Jerry M. Harris [b]

[a] *Institute of Geophysics, Chinese Academy of Sciences, Beijing 100101, China*
[b] *Department of Geophysics, Stanford University, Stanford, CA 94305, USA*

Received 29 November 1997; accepted 3 November 1998

Abstract

A finite difference method for the simulation of multi-component wavefield in viscous extensively dilatancy anisotropic (EDA) media is presented. Transformation of the stress and strain relation from frequency domain to time domain reveals that the viscous effect in EDA media is embedded into the terms of the third derivatives of the strain with respect to time. Numerical examples for viscous EDA media with dry and saturated cracks are calculated, respectively. In the calculation of the wavefields, the absorbing boundary conditions are used to suppress the artificial boundary reflection, the grid dispersion is suppressed by flux corrective transformation (FCT) technique. Snapshots and seismic records show that the existence of cracks and the material contents in the cracks exhibits significant influences on the wave propagation, especially on the radiation pattern and attenuated factor.

Keywords: Multi-component wavefield simulation; Extensively dilatancy anisotropic media; Flux corrective transformation

1. Introduction

Results from seismic exploration, seismic deep sounding, and earthquake seismology have shown that seismic anisotropy is widespread in the interiors of the earth. Seismic anisotropy can be induced by thin layering (e.g., Backus, 1962; Helbig, 1984; Thomsen, 1986; Schoenberg and Douma, 1988; Hsu and Schoenberg, 1993; Schoenberg and Muir, 1989), oriented cracks or fractures (e.g., Crampin, 1981; Hudson, 1981; Liu et al., 1993) and inhomogeneity (e.g., Grechka and McMechan, 1995). It is well-known that the study of oriented cracks or fractures is very important for reservoir description and characterization, because cracks or fractures not only may be the location of oil or gas reservoir, but also be the pathway of the oil and gas transportation. Maybe this is the reason why so many seismologists put their attention to the study of cracks or fractures. For example, Crampin (1981) and Hudson (1981) obtained an apparent constitute relationship for such a cracked medium, and Crampin (1984) developed the EDA (extensively dilatancy anisotropy) model. In practice, the EDA model can be used to interpret the shear wave splitting observed in surface, VSP, cross-hole, and other seismic data.

* Corresponding author. Fax: +86-10-6487-1995; E-mail: zjzhang@mail.c-geos.ac.cn

0031-9201/99/$ - see front matter
PII: S0031-9201(99)00043-6

In the last few years, seismic propagation in non-elastically isotropic and anisotropic media was studied. Kosik (1993) studied non-linear seismic waves in an elastic and isotropic media, Carcione (1988, 1990, 1994) and Booth and Crampin (1983a,b) investigated the wave propagation and the influence of non-elasticity on the wave velocities in dissipate and anisotropic media. Crampin (1978) obtained effective elastic constants by modeling the variation of wave velocities in cracked solids with a first-order approximation theory by Garbin and Knopoff (1973) and Garbin and Knopoff (1975a,b). Hudson developed a more general approach to calculating the elastic constants of cracked solids, which includes the first-order (Hudson, 1981) and second-order (Hudson, 1982) scattering interactions. Furthermore, Crampin (1981) and Hudson (1981) used the complex elastic constants to represent wave attenuation and demonstrated how to calculate velocity and attenuation variations in media with aligned cracks. The theoretical studies by Crampin, Hudson and others showed that the attenuation, compared to velocity, is more sensitive to the existence of oriented cracks and the material contents in the cracks. Different techniques have been developed to interpret various seismic data. For example, Queen and Rizer (1990) and Liu et al. (1993) studied the anisotropic effects on traveltime and polarization for cross-hole and reverse VSP data in cracked and fractured media. But few results about the non-elastic effects on traveltime, polarization, and other wave properties in EDA media were published. In this paper, we present a finite difference method to simulate seismic waves in heterogeneous non-elastic EDA media. We first present some results about the EDA constitute relationship in time domain, then introduce the forward modeling scheme of finite difference method, the treatments of the grid dispersion and the artificial boundary reflection. Some examples for the models without cracks, with dry or saturated cracks are calculated to investigate the effects of cracks, and material contents on the wave propagation.

1.1. Elastodynamic equation in viscous EDA media

In frequency domain, the elastic constants of EDA media, which include the non-elasticity caused by the existence of oriented cracks and inclusive materials in the cracks, are described as (Crampin, 1981; Hudson, 1981):

$$\mathbf{C} = C^{\mathrm{R}} + i\omega^3 C^{\mathrm{I}} \tag{1}$$

where, $\mathbf{C} = \{C_{ijkl}\}$ $(i,j,k,l = 1,2,3)$ is a complex elastic parameter matrix, ω is the angular frequency, and $i = \sqrt{-1}$ for the sign i before $\omega^3 C^{\mathrm{I}}$ in the above equation. Here, the real part of these elastic constants can be expressed in a perturbation form:

$$C^{\mathrm{R}} = \left\{C^0_{ijkl}\right\} + \left\{C^1_{ijkl}\right\} + \left\{C^2_{ijkl}\right\}, \tag{2}$$

and the imaginary part omitting the term of ω^3 can be approximated by the following formula:

$$\{C^{\mathrm{I}}_{ijkl}\} = \begin{bmatrix} C_{11}/C_0 & A & A & 0 & 0 & 0 \\ A & C_{22}/D_0 & B & 0 & 0 & 0 \\ A & B & C_{22}/D_0 & 0 & 0 & 0 \\ 0 & 0 & 0 & 0 & 0 & 0 \\ 0 & 0 & 0 & 0 & C_{55}/F & 0 \\ 0 & 0 & 0 & 0 & 0 & C_{11}/F \end{bmatrix}. \tag{3}$$

In Eq. (2), C^0_{ijkl} represents the elastic properties of the medium surrounded the crack, and C^1_{ijkl} and C^2_{ijkl} are the first and second perturbations induced by the existence of oriented cracks and the inclusive materials in cracks. Explicit expressions of these parameters and constants A, B, C_0, D_0, E, F are given in Appendix A.

We can transform Eq. (1) from frequency domain into time domain, and obtain the following constitutive relationship as follows:

$$C = C^{\mathrm{R}} - C^{\mathrm{I}} \frac{\partial^3}{\partial t^3}. \tag{4}$$

Then, the wave equation for non-elastic EDA media can be expressed in time domain as:

$$\frac{\partial^2 U_i}{\partial t^2} = \frac{\partial}{\partial x_j}\left(C^{\mathrm{R}}_{ijkl}\frac{\partial U_k}{\partial x_l}\right) - \frac{\partial}{\partial x_j}\left(C^{\mathrm{I}}_{ijkl}\frac{\partial^4 U_k}{\partial t^3 \partial x_l}\right) + F_i \tag{5}$$

where, F_i, denotes the force component in x_i direction ($x_i = x$, y, z, z for $i = 1$, 2, 3) (Zhang et al., 1998).

When we study the 2-D wavefields in x–z plane, Eq. (5) can be written as:

$$\begin{aligned}
&\rho(x,z)\frac{\partial^2}{\partial t^2}U(x,z,t)\\
&\quad=\frac{\partial}{\partial x}\left[\mathbf{B}_{\mathrm{R}}(x,z)\frac{\partial}{\partial x}U(x,z,t)\right]\\
&\qquad+\frac{\partial}{\partial x}\left[\mathbf{D}_{\mathrm{R}}(x,z)\frac{\partial}{\partial z}U(x,z,t)\right]\\
&\qquad+\frac{\partial}{\partial z}\left[\mathbf{E}_{\mathrm{R}}(x,z)\frac{\partial}{\partial x}U(x,z,t)\right]\\
&\qquad+\frac{\partial}{\partial z}\left[\mathbf{G}_{\mathrm{R}}(x,z)\frac{\partial}{\partial z}U(x,z,t)\right]\\
&\qquad+\frac{\partial}{\partial x}\left[\mathbf{B}_{\mathrm{R}}(x,z)\frac{\partial^4}{\partial x\partial t^3}U(x,z,t)\right]\\
&\qquad+\frac{\partial}{\partial x}\left[\mathbf{D}_{\mathrm{R}}(x,z)\frac{\partial^4}{\partial z\partial t^3}U(x,z,t)\right]\\
&\qquad+\frac{\partial}{\partial z}\left[\mathbf{E}_{\mathrm{I}}(x,z)\frac{\partial^4}{\partial x\partial t^3}U(x,z,t)\right]\\
&\qquad+\frac{\partial}{\partial z}\left[\mathbf{G}_{\mathrm{I}}(x,z)\frac{\partial^4}{\partial z\partial t^3}U(x,z,t)\right] \qquad (6)
\end{aligned}$$

where, x, z and t are Cartesian coordinates and time variable, respectively. The $\rho(x,z)$ is density of the media. $\mathbf{U}(x,z,t)=[U_x(x,z,t),U_y(x,z,t),U_z(x,z,t)]^{\mathrm{T}}$, $U_x(x,z,t)$, $U_y(x,z,t)$ and $U_z(x,z,t)$ are displacement components in x, y and z directions, respectively. $\mathbf{F}=[F_x(x,z,t),F_y(x,z,t),F_z(x,z,t)]^{\mathrm{T}}$ is the force matrix. $\mathbf{B}_{\mathrm{R}}(x,z)$, $\mathbf{D}_{\mathrm{R}}(x,z)$, $\mathbf{E}_{\mathrm{R}}(x,z)$, $\mathbf{G}_{\mathrm{R}}(x,z)$, $\mathbf{B}_{\mathrm{I}}(x,z)$, $\mathbf{D}_{\mathrm{I}}(x,z)$, $\mathbf{E}_{\mathrm{I}}(x,z)$ and $\mathbf{G}_{\mathrm{I}}(x,z)$ are the matrices consisted of real and imaginary part of the elastic parameters C_{ij} $(i,j=1,2,\ldots,6)$.The corresponding relationship between C_{ij}, and C_{ijkl} can be seen in the works of Crampin (1981) and others, and in

$$\mathbf{B}_{\mathrm{R}}(x,z)=\begin{bmatrix}C_{11}^{\mathrm{R}} & C_{15}^{\mathrm{R}} & C_{16}^{\mathrm{R}}\\ C_{15}^{\mathrm{R}} & C_{55}^{\mathrm{R}} & C_{56}^{\mathrm{R}}\\ C_{16}^{\mathrm{R}} & C_{56}^{\mathrm{R}} & C_{66}^{\mathrm{R}}\end{bmatrix}\quad\mathbf{D}_{\mathrm{R}}(x,z)=\begin{bmatrix}C_{15}^{\mathrm{R}} & C_{13}^{\mathrm{R}} & C_{14}^{\mathrm{R}}\\ C_{55}^{\mathrm{R}} & C_{35}^{\mathrm{R}} & C_{45}^{\mathrm{R}}\\ C_{66}^{\mathrm{R}} & C_{36}^{\mathrm{R}} & C_{46}^{\mathrm{R}}\end{bmatrix}$$

$$\mathbf{E}_{\mathrm{R}}(x,z)=\begin{bmatrix}C_{15}^{\mathrm{R}} & C_{55}^{\mathrm{R}} & C_{56}^{\mathrm{R}}\\ C_{13}^{\mathrm{R}} & C_{35}^{\mathrm{R}} & C_{36}^{\mathrm{R}}\\ C_{14}^{\mathrm{R}} & C_{45}^{\mathrm{R}} & C_{46}^{\mathrm{R}}\end{bmatrix}\quad\mathbf{G}_{\mathrm{R}}(x,z)=\begin{bmatrix}C_{55}^{\mathrm{R}} & C_{35}^{\mathrm{R}} & C_{45}^{\mathrm{R}}\\ C_{35}^{\mathrm{R}} & C_{33}^{\mathrm{R}} & C_{34}^{\mathrm{R}}\\ C_{45}^{\mathrm{R}} & C_{34}^{\mathrm{R}} & C_{44}^{\mathrm{R}}\end{bmatrix}$$

$$\mathbf{B}_{\mathrm{I}}(x,z)=\begin{bmatrix}C_{11}^{\mathrm{I}} & C_{15}^{\mathrm{I}} & C_{16}^{\mathrm{I}}\\ C_{15}^{\mathrm{I}} & C_{55}^{\mathrm{I}} & C_{56}^{\mathrm{I}}\\ C_{16}^{\mathrm{I}} & C_{56}^{\mathrm{I}} & C_{66}^{\mathrm{I}}\end{bmatrix}\quad\mathbf{D}_{\mathrm{I}}(x,z)=\begin{bmatrix}C_{15}^{\mathrm{I}} & C_{13}^{\mathrm{I}} & C_{14}^{\mathrm{I}}\\ C_{55}^{\mathrm{I}} & C_{35}^{\mathrm{I}} & C_{45}^{\mathrm{I}}\\ C_{66}^{\mathrm{I}} & C_{36}^{\mathrm{I}} & C_{46}^{\mathrm{I}}\end{bmatrix}$$

$$\mathbf{E}_{\mathrm{I}}(x,z)=\begin{bmatrix}C_{15}^{\mathrm{I}} & C_{55}^{\mathrm{I}} & C_{56}^{\mathrm{I}}\\ C_{13}^{\mathrm{I}} & C_{35}^{\mathrm{I}} & C_{36}^{\mathrm{I}}\\ C_{14}^{\mathrm{I}} & C_{45}^{\mathrm{I}} & C_{46}^{\mathrm{I}}\end{bmatrix}\quad\mathbf{G}_{\mathrm{I}}(x,z)=\begin{bmatrix}C_{55}^{\mathrm{I}} & C_{35}^{\mathrm{I}} & C_{45}^{\mathrm{I}}\\ C_{35}^{\mathrm{I}} & C_{33}^{\mathrm{I}} & C_{34}^{\mathrm{I}}\\ C_{45}^{\mathrm{I}} & C_{34}^{\mathrm{I}} & C_{44}^{\mathrm{I}}\end{bmatrix}.$$

2. Finite difference modeling scheme in viscous EDA media

By discretizing Eq. (6) with finite difference technique, we can obtain the discretized formula for the simulation of three component wavefields in viscous EDA media:

$$\begin{aligned}
&\mathbf{U}(i,j,n+1)\\
&\quad=2\mathbf{U}(i,j,n)-\mathbf{U}(i,j,n-1)\\
&\qquad+\frac{(\Delta t)^2}{\rho(\Delta x)^2}\left\{\mathbf{B}_{\mathrm{R}}\left(i+\frac{1}{2},j\right)\left[\mathbf{U}(i+1,j,n)\right.\right.\\
&\qquad\left.-\mathbf{U}(i,j,n)\right]-\mathbf{B}_{\mathrm{R}}\left(i-\frac{1}{2},j\right)\left[\mathbf{U}(i,j,n)\right.\\
&\qquad\left.\left.-\mathbf{U}(i-1,j,n)\right]\right\}+\frac{(\Delta t)^2}{\rho(\Delta x\Delta z)}\left\{\mathbf{D}_{\mathrm{R}}(i+1,j)\right.\\
&\qquad\times\left[\mathbf{U}(i+1,j+1,n)-\mathbf{U}(i+1,j-1,n)\right]\\
&\qquad-\mathbf{D}_{\mathrm{R}}(i-1,j)\left[\mathbf{U}(i-1,j+1,n)\right.\\
&\qquad\left.-\mathbf{U}(i-1,j-1,n)\right]+\mathbf{E}_{\mathrm{R}}(i,j+1)\\
&\qquad\times\left[\mathbf{U}(i+1,j+1,n)-\mathbf{U}(i-1,j+1,n)\right]\\
&\qquad-\mathbf{E}_{\mathrm{R}}(i,j-1)\left[\mathbf{U}(i+1,j-1,n)\right.\\
&\qquad\left.\left.-\mathbf{U}(i-1,j-1,n)\right]\right\}\\
&\qquad+\frac{(\Delta t)^2}{\rho(\Delta z)^2}\left\{\mathbf{G}_{\mathrm{R}}(i,j+1)\right.\\
&\qquad\times\left[\mathbf{U}(i,j+1,n)-\mathbf{U}(i,j,n)\right]-\mathbf{G}_{\mathrm{R}}\left(i,j-\frac{1}{2}\right)\\
&\qquad\left.\times\left[\mathbf{U}(i,j,n)-\mathbf{U}(i,j-1,n)\right]\right\}+\frac{(\Delta t)^2}{\rho(\Delta x)^2}\\
&\qquad\times\left\{\mathbf{B}_{\mathrm{I}}\left(i+\frac{1}{2},j\right)\left[V(i+1,j,n)-V(i,j,n)\right]\right.\\
&\qquad\left.-\mathbf{B}_{\mathrm{I}}\left(i-\frac{1}{2},j\right)\left[V(i,j,n)-\mathbf{U}(i-1,j,n)\right]\right\}\\
&\qquad+\frac{(\Delta t)^2}{\rho(\Delta x\Delta z)}\left\{\mathbf{D}_{\mathrm{I}}(i+1,j)\left[V(i+1,j+1,n)\right.\right.
\end{aligned}$$

$$
\begin{aligned}
&- V(i+1,j-1,n)\big] - \mathbf{D}_1(i-1,j)\\
&\times\big[V(i-1,j+1,n) - V(i-1,j-1,n)\big]\\
&+ \mathbf{E}_1(i,j+1)\big[V(i+1,j+1,n)\\
&- V(i-1,j+1,n)\big] - \mathbf{E}_1(i,j-1)\\
&\times\big[V(i+1,j-1,n) - V(i-1,j-1,n)\big]\big\}\\
&+ \frac{(\Delta t)^2}{\rho(\Delta z)^2}\left\{\mathbf{G}_1(i,j+1)\big[V(i,j+1,n)\right.\\
&\left.- V(i,j,n)\big] - \mathbf{G}_1\left(i,j-\frac{1}{2}\right)\big[V(i,j,n)\big]\right\}\\
&+ \boldsymbol{F}(i,j,n) \qquad (7)
\end{aligned}
$$

with the following initial conditions

$$\mathbf{U}(x,z,t=0) = [0,0,0]^{\mathrm{T}},$$

$$\dot{\mathbf{U}}(x,z,t=0) = [0,0,0]^{\mathrm{T}} \qquad (8)$$

where, $\mathbf{U}(i,j,n) = \mathbf{U}(i\Delta x, j\Delta z, n\Delta t)$ is the discretized displacement component matrix $[U_x(i\Delta x, j\Delta z, n\Delta t, U_y(i\Delta x, j\Delta z, n\Delta t, U_z(i\Delta x, j\Delta z, n\Delta t)]^{\mathrm{T}}$, $V(i,j,n) = V(i\Delta x, j\Delta z, n\Delta t)$ are the discretized third derivatives of the displacement component with respect to time t, namely, $[\ddot{u}_x(i\Delta x, j\Delta z, n\Delta t, \ddot{u}_y(i\Delta x, j\Delta z, n\Delta t), \ddot{u}_z(i\Delta x, j\Delta z, n\Delta t)]^{\mathrm{T}}$. $\boldsymbol{F}(i,j,n) = \boldsymbol{F}(i\Delta x, j\Delta z, n\Delta t)$ are the vectors consisted of three force source components in x, y and z direction, namely, $[f_x(i\Delta x, j\Delta z, n\Delta t), f_y(i\Delta x, j\Delta z, n\Delta t), U_z(i\Delta x, j\Delta z, n\Delta t)]^{\mathrm{T}}$, Δx, Δz and Δt are the spatial and temporal increments, respectively.

The value of $V(i,j,n)$ in Eq. (7) is calculated using the acceleration components of particle motion, i.e.,

$$V(i,j,n) = \frac{\ddot{U}(i,j,n) - \ddot{U}(i,j,n-1)}{\Delta t} \qquad (9)$$

with the initial conditions

$$\ddot{U}(x,z,t=0) = \dddot{U}(x,z,t=0) = [0,0,0]^{\mathrm{T}}. \qquad (10)$$

Therefore, we can calculate three-component wavefield at $t_{n+1} = (n+1)\Delta t$ from the wavefields at $t_n = n\Delta t$ and $t_{n-1} = (n-1)\Delta t$ by combining Eq. (7) with initial condition Eqs. (8)–(10). Repeating this process, we can obtain the complete synthetic seismograms.

3. Artificial boundary treatment

As the limitation of computer memory, we can only calculate the seismic wavefields within limited zone. We need to handle the artificial boundaries in the numerical computation. These boundaries can create the artificial reflections. The reflections on artificial boundaries should be eliminated. In this

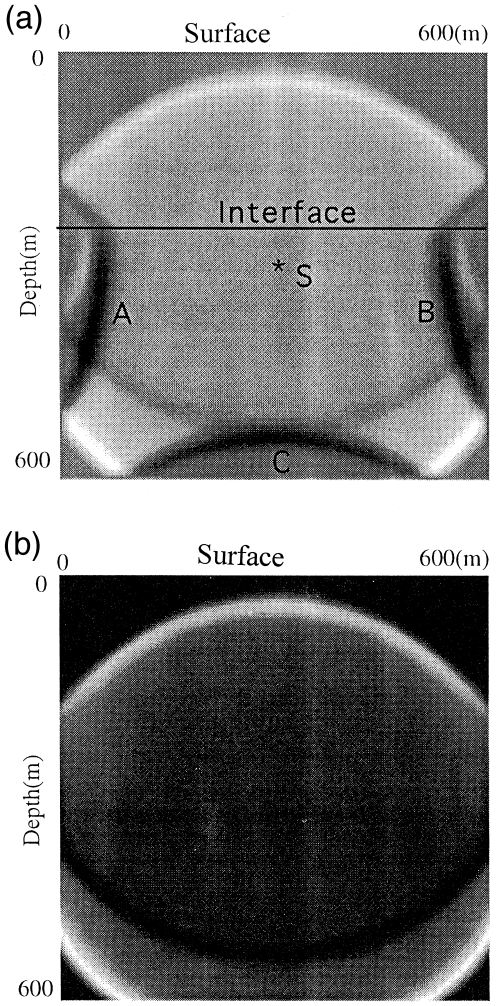

Fig. 1. Snapshots of y component wavefield. (a) Without the treatment of artificial boundary reflection. The wavefront events A, B and C are the reflections on the left, right and bottom (artificial) boundaries. (b) After the treatment of artificial boundary reflection, the reflection events A, B and C are suppressed effectively.

work, we assume that the media at the artificial boundaries are elastically anisotropic, and use the following method to suppress the artificial reflections. The detailed derivations can be found in the works of Zhang et al. (1993), He and Zhang (1996) and Yang (1996):

$$\left(\vec{\mathbf{I}}\frac{\partial}{\partial t}+\rho^{-\frac{1}{2}}\vec{\mathbf{R}}^{\frac{1}{2}}\frac{\partial}{\partial x}\right)\vec{\mathbf{U}}=0 \quad \text{for the right boundary,} \tag{11}$$

$$\left(\vec{\mathbf{I}}\frac{\partial}{\partial t}+\rho^{-\frac{1}{2}}\vec{\mathbf{R}}^{\frac{1}{2}}\frac{\partial}{\partial x}\right)\vec{\mathbf{U}}=0 \quad \text{for the left boundary,} \tag{12}$$

$$\left(\vec{\mathbf{I}}\frac{\partial}{\partial t}+\rho^{-\frac{1}{2}}\vec{\mathbf{B}}^{\frac{1}{2}}\frac{\partial}{\partial x}\right)\vec{\mathbf{U}}=0$$

for the bottom boundary, (13)

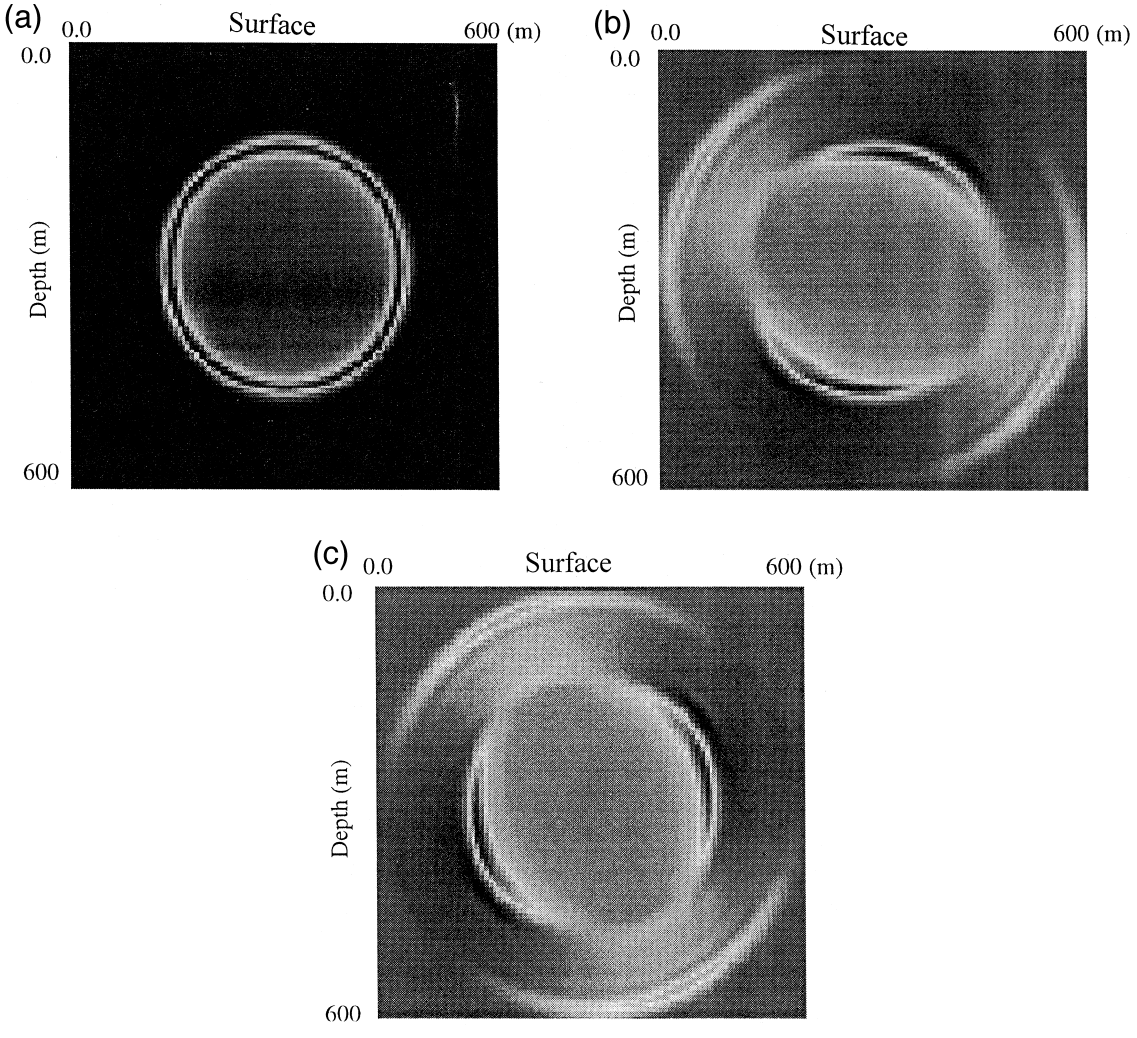

Fig. 2. Snapshots of x, y and z component wavefields in homogeneous isotropic media. (a) The x component slice, (b) y component slice, (c) z component slice after the propagation for 0.08 s from the source position.

where matrices $\vec{\mathbf{R}}$ and $\vec{\mathbf{B}}$ have the following forms for generally anisotropic media:

$$\vec{\mathbf{R}} = \begin{pmatrix} C_{11} & C_{16} & C_{15} \\ C_{16} & C_{66} & C_{56} \\ C_{15} & C_{56} & C_{55} \end{pmatrix} \quad \vec{\mathbf{B}} = \begin{pmatrix} C_{55} & C_{45} & C_{35} \\ C_{45} & C_{44} & C_{34} \\ C_{35} & C_{34} & C_{33} \end{pmatrix}$$

Fig. 1a–b are the snapshots of component without and with the treatment of artificial boundary for a model with two layers, respectively. From the snapshots, we can see that the above absorbing conditions work well at the artificial boundaries, and the artificial reflections have been suppressed effectively.

4. Grid dispersion treatment

In the computation of wavefields, grid dispersion would happen. Increasing grid number within individual wavelength can reduce dispersion effects, but requires more inner memory of the computer. The flux corrective transportation (FCT) technique was developed (Boore, 1972a,b; Yang, 1996; and others) and successfully applied to suppress the grid dispersion when we solve large gradient problems in discretized domain. Here, we extended the FCT technique to treat the grid dispersion in the modeling of seismic waves in anisotropic media.

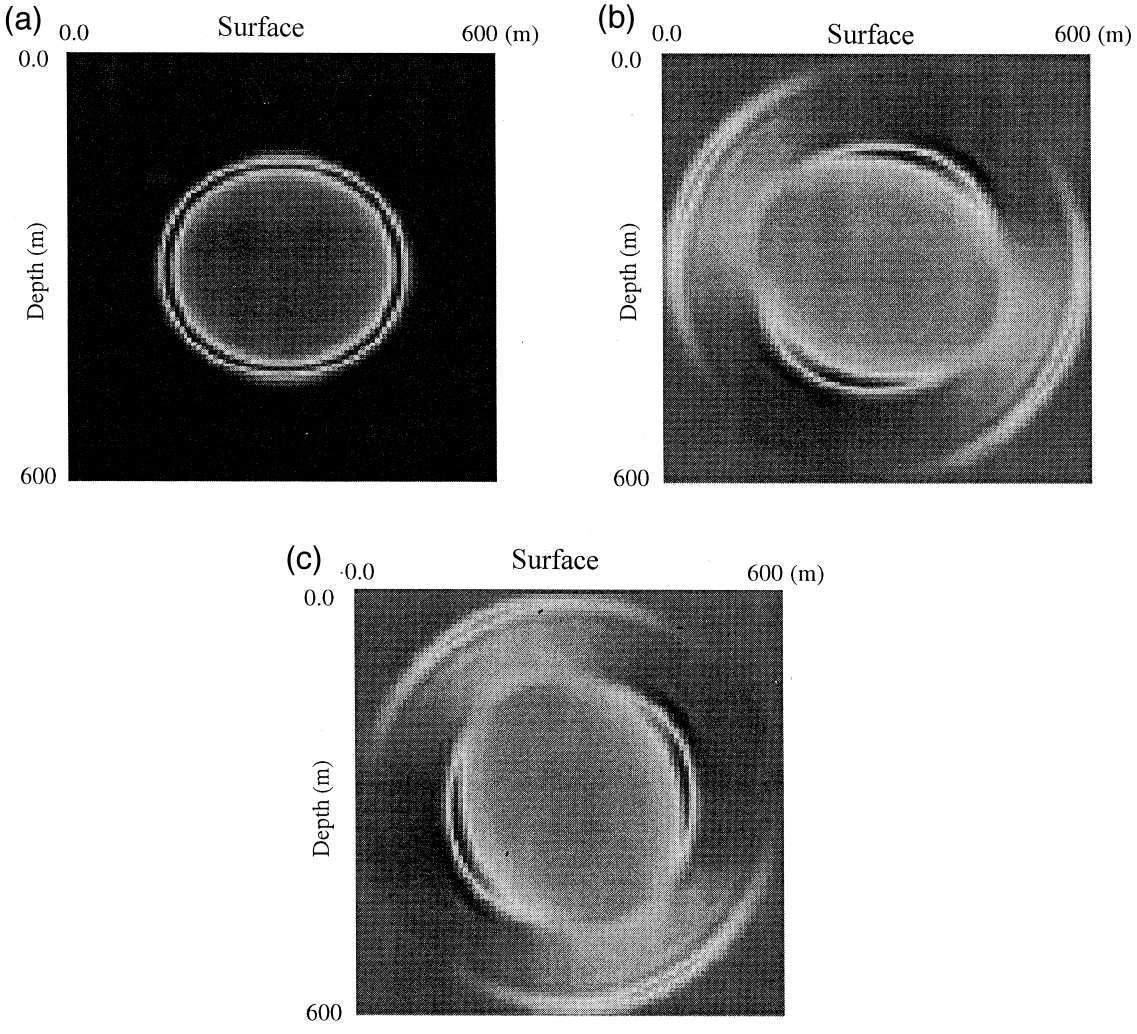

Fig. 3. Snapshots of x, y and z component wavefields in elastic EDA media with dry cracks. (a) The x component slice, (b) y component slice, (c) z component slice after the propagation for 0.08 s from the source position.

After each step of wavefield computation, we can eliminate the grid dispersion effects by following procedures:

1. calculate diffusion flux and smooth the numerical solutions of finite difference equations at the n-th step;
2. calculate the diffusion flux and smooth the numerical solutions of finite difference equations at the $(n+1)$-th time step;
3. calculate the offsetting diffusion flux;
4. eliminate the effect of grid dispersion for the three component wavefields.

The detail about the processing technique of grid dispersion can be seen in Appendix B.

5. Computation and analyses

We use the finite difference method developed above to simulate multi-component seismic wave-

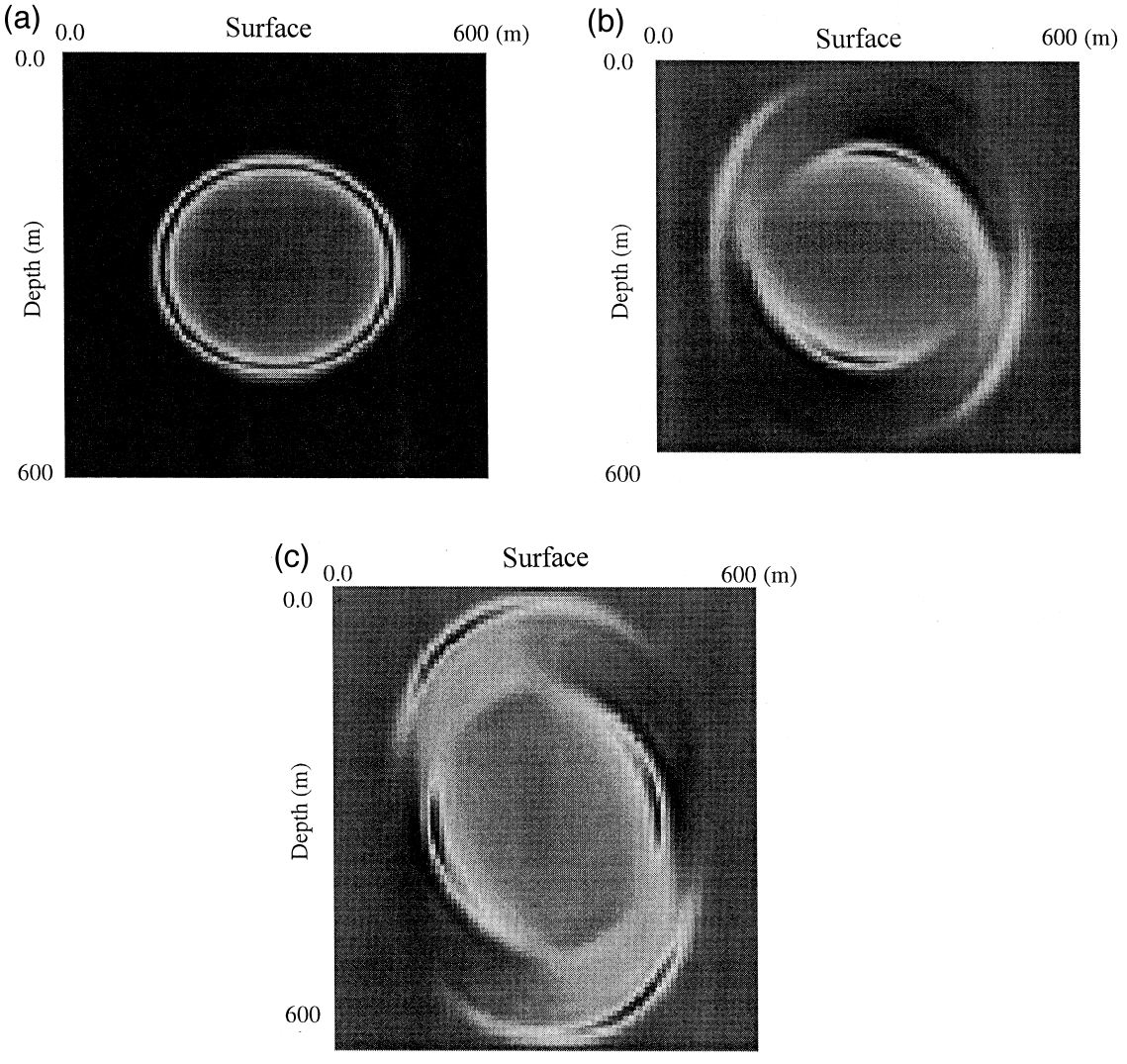

Fig. 4. Snapshots of x, y and z component wavefields in elastic EDA media with water saturated cracks. (a) The x component slice, (b) y component slice, (c) z component slice after the propagation for 0.08 s from the source position.

fields in viscous EDA media. In the following examples, they have the same the model geometrical parameters, namely, the grid numbers of the model are $N_x = N_z = 101$, $\mathrm{d}x = \mathrm{d}z = 0.006$ km, $\mathrm{d}t = 0.0004$ s. The source is located at the node of (51, 51).

5.1. Isotropic model

For the isotropic model, the velocities for P and S waves are 3.0 and $1/73$ km/s, respectively. The snapshots of P, SV and SH waves are shown in Fig. 2a–c. It can be seen that the wavefronts of these

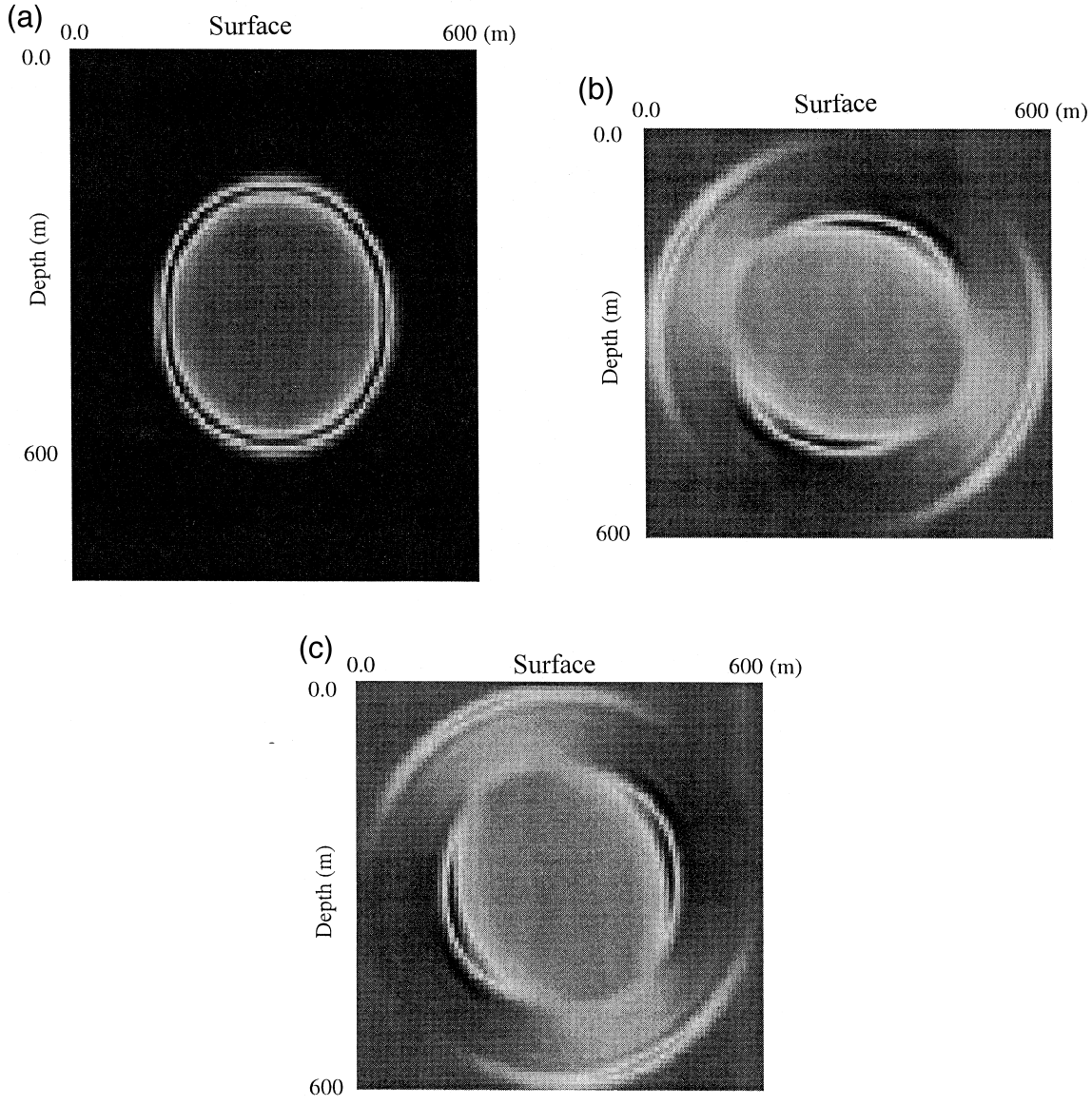

Fig. 5. Snapshots of x, y and z component wavefields in non-elastic EDA media with dry cracks. (a) The x component slice, (b) y component slice, (c) z component slice after the propagation for 0.08 s from the source position.

waves are circular and isotropic. The dispersion effect after grid dispersion treatment is very weak.

5.2. Elastic EDA model

For the elastic EDA model, we consider the media with dry cracks and water saturated cracks, respectively. The velocities of P and S waves for the surrounding rock of cracks are 3.0 and 1.73 km/s. The crack density is 0.1 crack ratio $d = 0.001$. We do not consider the effect of non-elasticity in the calculation of wavefield here. Fig. 3a–c are the three component seismic snapshots at 200th step in the isotropic media without cracks. Fig. 4a–c are the multi-component seismic snapshots at 200th step in EDA media without the consideration of viscous effects. The snapshots of qP, qSV and qSH waves

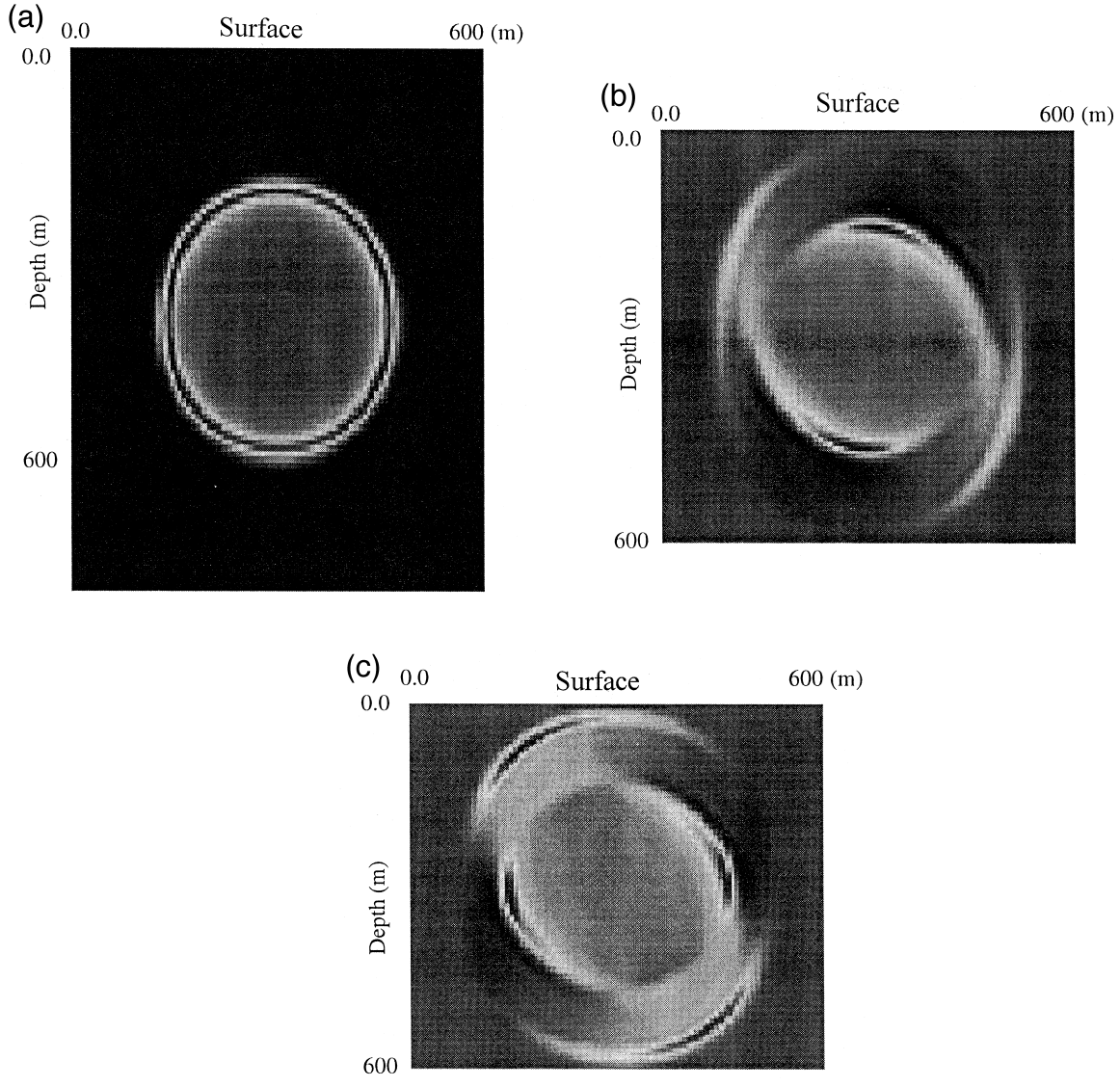

Fig. 6. Snapshots of x, y and z component wavefields in non-elastic EDA media with water saturated cracks. (a) The x component slice, (b) y component slice, (c) z component slice after the propagation for 0.08 s from the source position.

show that the seismic velocities depend on the propagating direction. The difference of seismic velocity between qSV and qSH wave can be clearly seen. The existence of oriented cracks cause shear wave splitting, but the effects of material content in cracks on seismic propagation are not significant.

5.3. Viscous EDA model

For the viscous EDA model, we also consider the media with dry cracks and water saturated cracks, respectively. The models are same as the above ones, but we consider the effect of non-elasticity. Figs. 5a–c and 6a–c are the multi-component seismic snapshots at 200th step in EDA media for dry cracks and water saturated cracks under the consideration of viscous effects, respectively. By the analysis of the seismograms calculated for the models of elastic and non-elastic EDA media (Figs. 7 and 8), we can see that, in addition to the phenomenon of shear wave splitting, the seismic waveforms are widen, and the amplitude of qSV and qSH waves are attenuated much more fast than the qP-wave. Meanwhile, the radiation pattern exhibits some changes for qP and qSV waves in media with dry and saturated cracks, but no change for qSH wave exists, because of the

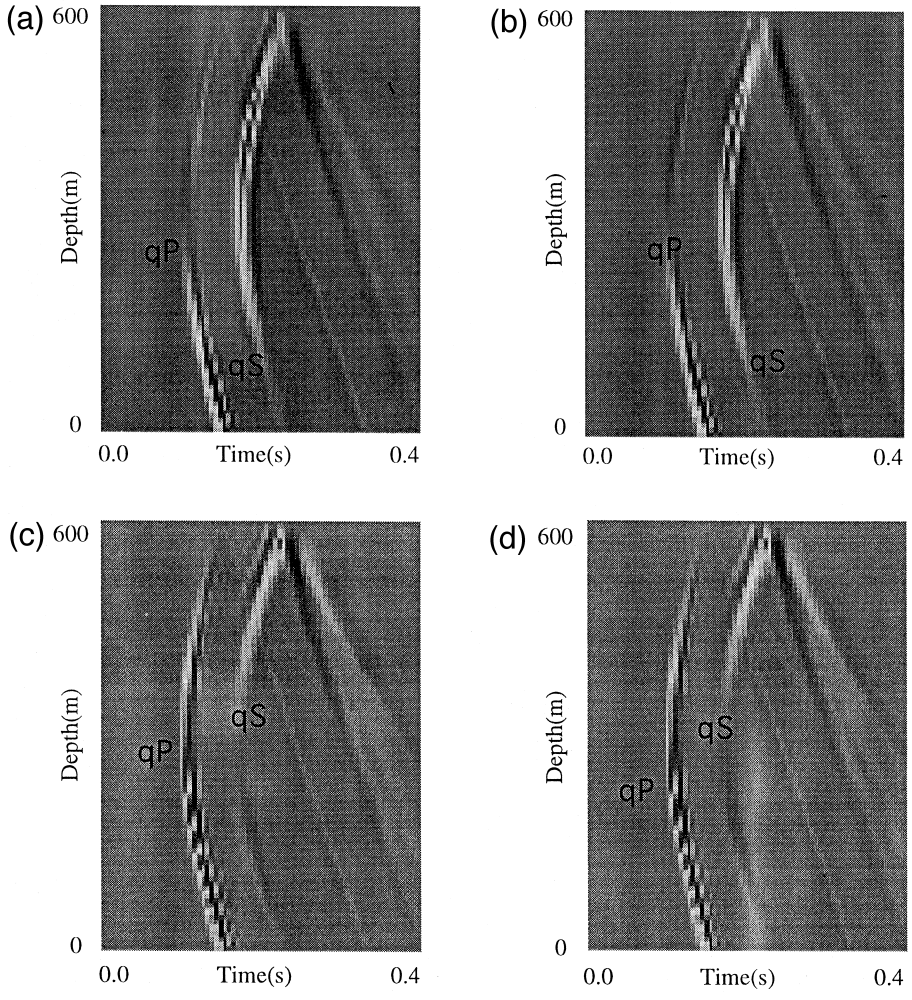

Fig. 7. VSP seismograms for elastic EDA media and non-elastic EDA media with dry cracks. (a) The x component record, (b) z component record for elastic EDA model, (c) x component record, (d) z component record for non-elastic EDA model.

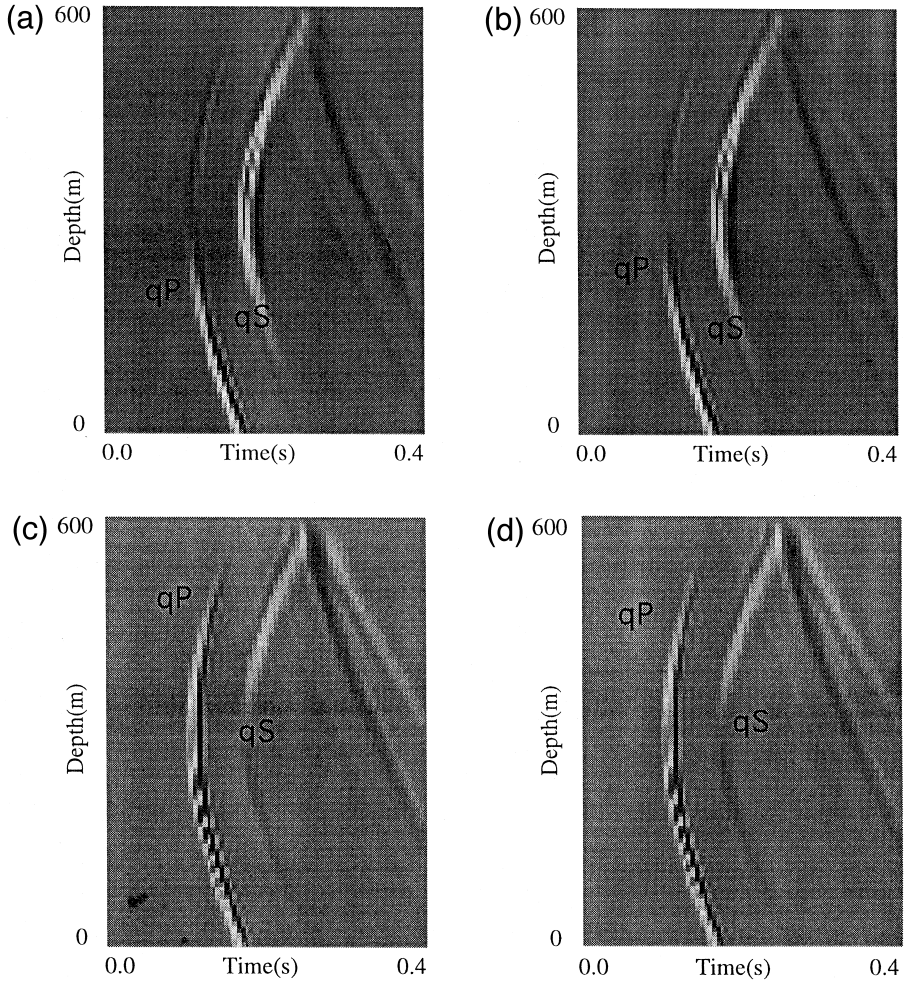

Fig. 8. VSP seismograms for elastic EDA media and non-elastic EDA media with water saturated cracks. (a) The x component record, (b) z component record for elastic EDA model, (c) x component record, (d) z component record for non-elastic EDA model.

assumption of vertical oriented cracks in their surrounding rock. This means the attenuating effects are good indicator of inclusive materials (oil, gas or other kind of material) in cracks.

6. Conclusions

The finite difference method for the simulation of multi-component seismic wavefields in viscous EDA media is presented. The viscous effect in EDA media can be embedded in the terms of the third derivatives of the strain with respect to time. In the calculation of multi-component wavefields, the artificial boundary reflections are suppressed with absorbing boundary conditions, and the grid dispersions is effectively treated with FCT technique. The stress continuity condition at inner interface is kept using the FBI technique (Zhang et al., 1996). The computation shows that, the existence of oriented cracks or fractures would give rise to the phenomenon of shear-wave splitting; with the consideration of viscosity, seismic waveform will widen, radiating pattern is different from the elastic cases, the attenuation of seismic waves are also anisotropic; the content in the cracks have significant effects on the radiating pat-

terns; attenuation is more sensitive than velocity to the existence of the crack, especially to the content in the cracks.

Acknowledgements

The first author would like to thank the financial support from Chinese Natural Sciences Foundation, the President Foundation of Chinese Academy of Sciences, and the National Key Lab. Foundation in Chengdu Science and Technology College. The first author is also thankful to the support of computing resources for this work from STP, Department of Geophysics, Stanford University. The comments and help from Dr. Enru Liu from Edinburg Geology Survey and Dr. J. Queen from MIT and Dr. G.Y. Wang from Stanford University are also appreciated. The constructive comments and suggestion from Prof. Irina O. Bayuk and another anonymous reviewer are greatly appreciated.

Appendix A

For a weak distribution of parallel penny-shaped cracks, normal to the x direction, with crack density $\varepsilon = Na^3/v$ ($\varepsilon \ll 1$), where N is the number of cracks of radius a in volume v in an isotropic solid with Lame constants λ, and μ. Hudson (1981, 1982) showed that the general expression for effective elastic constants $\{C_{ijkl}\}$ applicable to the propagation of long-wavelength seismic waves through a cracked solid is:

$$\{C_{ijkl}\} = \{C^0_{ijkl}\} + \{C^1_{ijkl}\} + \{C^2_{ijkl}\}$$

where $\{C^1_{ijkl}\}$ is the first order and $\{C^2_{ijkl}\}$ is the second order perturbation of the isotropic elastic constants $\{C^0_{ijkl}\}$ of the solid without crack.

$$\{C^0_{ijkl}\} = \begin{bmatrix} \lambda+2\mu & \lambda & \lambda & 0 & 0 & 0 \\ \lambda & \lambda+2\mu & \lambda & 0 & 0 & 0 \\ \lambda & \lambda & \lambda+2\mu & 0 & 0 & 0 \\ 0 & 0 & 0 & \mu & 0 & 0 \\ 0 & 0 & 0 & 0 & \mu & 0 \\ 0 & 0 & 0 & 0 & 0 & \mu \end{bmatrix}$$

$$\{C^1_{ijkl}\} = -\frac{\varepsilon}{\mu} \times \begin{bmatrix} (\lambda+2\mu)^2 & \lambda(\lambda+2\mu) & \lambda(\lambda+2\mu) & 0 & 0 & 0 \\ \lambda(\lambda+2\mu) & \lambda^2 & \lambda^2 & 0 & 0 & 0 \\ \lambda(\lambda+2\mu) & \lambda^2 & \lambda^2 & 0 & 0 & 0 \\ 0 & 0 & 0 & \mu^2 & 0 & 0 \\ 0 & 0 & 0 & 0 & \mu^2 & 0 \\ 0 & 0 & 0 & 0 & 0 & \mu^2 \end{bmatrix} \mathbf{D}$$

$$\{C^2_{ijkl}\} = -\frac{\varepsilon^2}{15} \times \begin{bmatrix} (\lambda+2\mu)q & \lambda q & \lambda q & 0 & 0 & 0 \\ \lambda q & \lambda^2 q/(\lambda+2\mu) & \lambda^2 q/(\lambda+2\mu) & 0 & 0 & 0 \\ \lambda q & \lambda^2 q/(\lambda+2\mu) & \lambda^2 q/(\lambda+2\mu) & 0 & 0 & 0 \\ 0 & 0 & 0 & x & 0 & 0 \\ 0 & 0 & 0 & 0 & x & 0 \\ 0 & 0 & 0 & 0 & 0 & x \end{bmatrix} \mathbf{D}^2$$

where $q = 15(\lambda/\mu)^2 + 28\lambda/\mu + 28$, $x = 2\mu(3\lambda + 8\mu)/(\lambda + 2\mu)$. The trace of the matrix $\mathbf{D}$ is trace $(\mathbf{D}) = [U_{11}, U_{11}, U_{11}, 0, U_{33}, U_{33}]$, and $U_{11} = 4(\lambda + 2\mu)/[3(\lambda + \mu)(1 + k)]$, $U_{33} = 16(\lambda + 2\mu)/[3(3\lambda + 4\mu)(1 + M)]$, $K = (\lambda' + 2\mu')(\lambda + 2\mu)/[\pi d\mu(\lambda + \mu)]$, $M = 4\mu'(\lambda + 2\mu)/[\pi d\mu(3\lambda + 4\mu)]$ and trace$(\mathbf{D}) = [U_{11}, U_{11}, U_{11}, 0, U_{33}, U_{33}]$, $X = [1.5 + (V_x/V_p)^5]U_{33}^2$,

$$Y = \left[2 + \frac{15}{4}\frac{V_s}{V_p} - 10\left(\frac{V_s}{V_p}\right)^3 + 8\left(\frac{V_s}{V_p}\right)^5\right]U_{11}^2.$$

Meanwhile, $\lambda = \rho(V_p^2 - 2V_s^2)$, $\lambda' = \rho'(V_p'^2 - 2V_s'^2)$, $\mu = \rho V_s^2$, $\mu' = \rho' V_s'^2$.

V_p and V_s are P and S waves velocity of rock surrounding crack. V_{p1} and V_{s1} are the P and S waves velocity of material inclusive in the cracks. ρ and ρ' are densities of the rock containing cracks and that of material inclusive in cracks. ε is the crack density, d and a are the ratio and radius of longer axis, respectively.

With the real parts of the complex elastic constants, we can calculate the imaginary part of elastic constants with Eq. (5), in which A, B, and other terms can be written as follows:

$$A = \left[(C_{1111} + C_{2222})/2 + C_{1122} + 2C_{1212}\right] /Q_1 - (C_{1111} + C_{2222})/2 - 2 + C^{\mathrm{I}}_{1212}$$

$$B = C^{\mathrm{I}}_{2222} - 2C^{\mathrm{I}}_{2323},$$

$$C_0 = 15\pi V_s^3/(Y\varepsilon\alpha^3),$$

$$D_0 = \frac{15\pi V_s V_p^3}{Y\varepsilon\alpha^3\left[\left(\frac{V_p}{V_s}\right)^2 - 2\right]^2}$$

$$F = 15\pi V_s^3/(\varepsilon X\alpha^3),$$

$$Q_1 = \frac{15\pi V_s V_p^3}{\varepsilon\alpha^3\left\{X + Y\left[\left(\frac{V_p}{V_s}\right)^2 - 1\right]^2\right\}}.$$

Appendix B

The FCT for the suppression of grid dispersion includes the following steps after obtaining the wavefields $\mathbf{U}(i,j,k)$, $\mathbf{U}(i,j,k+1)$ and $\mathbf{U}(i,j,k-1)$.

(1) Calculate diffusion flux and smooth the numerical solutions of finite difference equations at the n-th time step with the following expressions:

$$P\left(i+\frac{1}{2},j,k\right) = \eta_1\Big(\mathbf{U}(i+1,j,k) - \mathbf{U}(i,j,k) - \mathbf{U}(i+1,j,k-1) + \mathbf{U}(i,j,k-1)\Big)$$

$$Q\left(i,j+\frac{1}{2},k\right) = \eta_1\Big(\mathbf{U}(i,j+1,k) - \mathbf{U}(i,j,k) - \mathbf{U}(i,j+1,k-1) + \mathbf{U}(i,j,k-1)\Big) \times 0.008 \le \eta_1 \le 0.05$$

and

$$\tilde{U}(i,j,k+1) = \mathbf{U}(i,j,k+1) + \left(P\left(i+\frac{1}{2},j,k-1\right) - P\left(i-\frac{1}{2},j,k-1\right)\right) + \left(Q\left(i,j+\frac{1}{2},k-1\right) - Q\left(i,j+\frac{1}{2},k-1\right)\right).$$

(2) Calculate diffusion flux and smooth the numerical solutions of finite difference equations at the $(n+1)$-th time step. The diffusion flux components of x and z direction are:

$$\tilde{P}\left(i+\frac{1}{2},j,k+1\right) = \eta_2\Big(\tilde{U}(i+1,j,k+1) - \tilde{U}(i,j,k+1) - \tilde{U}(i+1,j,k) + \tilde{U}(i,j,k)\Big)$$

$$\tilde{Q}\left(i,j+\frac{1}{2},k+1\right) = \eta_2\Big(\tilde{U}(i,j+1,k+1) - \tilde{U}(i,j,k+1) - \tilde{U}(i,j+1,k) + \tilde{U}(i,j,k)\Big) \times 0.008 \le \eta_2 \le 0.05,$$

then, we can smooth the numerical solutions of finite difference equations with following expression:

$$\tilde{U}(i,j,k+1) = \mathbf{U}(i,j,k+1) + \left(\tilde{P}\left(i+\frac{1}{2},j,k-1\right) - \tilde{P}\left(i-\frac{1}{2},j,k-1\right)\right) + \left(\tilde{Q}\left(i,j+\frac{1}{2},k-1\right) - \tilde{Q}\left(i,j+\frac{1}{2},k-1\right)\right).$$

(3) Calculate the components of offsetting diffusion flux:

$$X\left(i+\frac{1}{2},j,k+1\right) = \tilde{U}(i+1,j,k+1) - \mathbf{U}(i+1,j,k) - \Big(\tilde{U}(i,j,k+1) - \mathbf{U}(i,j,k)\Big)$$

$$Y\left(i,j+\frac{1}{2},k+1\right) = \tilde{U}(i,j,+1,k+1) - \mathbf{U}(i,j+1,k) - \Big(\tilde{U}(i,j,k+1) - \mathbf{U}(i,j,k)\Big).$$

(4) Eliminate grid dispersion effects:

$$\mathbf{U}(i,j,k) = \tilde{U}(i,j,k+1) - \left(X\left(i+\frac{1}{2},j,k\right) - X\left(i-\frac{1}{2},j,k\right)\right) - \left(Y\left(i,j+\frac{1}{2},k\right) - Y\left(i,j-\frac{1}{2},k\right)\right).$$

References

Backus, G.E., 1962. Long-wave elastic anisotropy in a continental layering. J. Geophys. Res. 67, 4427–4440.

Boore, D.M., 1972. Finite-difference methods for seismic waves. In: Bolt, B.A. (Ed.), Methods in Computational Physics. Academic Press, New York, 11, 1–37.

Boore, D.M., 1972. Finite-difference methods for seismic wave propagation in heterogeneous materials. In: Bolt, B.A. (Ed.), Methods in Computational Physics. Academic Press, New York, 2, 21–22.

Booth, D.C., Crampin, S., 1983a. The anisotropic reflectivity technique: theory. Geophys. J. R. Astron. Soc. 72, 755–756.

Booth, D.C., Crampin, S., 1983b. The anisotropic reflectivity technique: anomalous arrives from an anisotropic upper mantle. Geophys. J. R. Astron. Soc. 72, 767–782.

Carcione, P., 1988. Wave propagation simulation in a linear-viscoelastic medium. Geophys. J. R. Astron. Soc. 93, 393–407.

Carcione, J.M., 1990. Wave propagation in anisotropic linear viscoelastic media: theory and simulated wavefields. Geophys. J. Int. 101, 739–750.

Carcione, J.M., 1994. Wavefronts in dissipative anisotropic media. Geophysics 59, 644–657.

Crampin, S., 1978. Seismic wave propagation through a cracked solid: polarization as a possible dilatancy diagnostic. Geophys. J. R. Astron. Soc. 53, 467–496.

Crampin, S., 1981. A review of wave motion in anisotropic and cracked elastic media. Wave Motion 3, 343–391.

Crampin, S., 1984. Effective anisotropic elastic constants for wave propagation through cracked solids. Geophys. J. R. Astron. Soc. 76, 135–145.

Garbin, H.D., Knopoff, L., 1973. The compressional modulus of a material permeated by a random distribution of free circular cracks. Q. Appl. Math. 3, 453–464.

Garbin, H.D., Knopoff, L., 1975a. The shear modulus of a material permeated by a random distribution of free circular cracks. Q. Appl. Math. 33, 296–300.

Garbin, H.D., Knopoff, L., 1975b. Elastic moduli of a medium with liquid-filled cracks. Q. Appl. Math. 33, 301–303.

Grechka, V.Y., McMechan, G.A., 1995. Is shear-wave splitting an indicator of seismic anisotropy? 65th Annu. Int. Meeting Soc. Explor. Geophys., Expanded Abstracts, 332–335.

He, Q., Zhang, Z., 1996. Seismic propagation and numerical simulation in transversely isotropic media (in Chinese). Jilin Univ. Press,

Helbig, K., 1984. Transverse isotropy in exploration seismology. Geophys. J. R. Astron. Soc. 76, 79–88.

Hsu, C.-J., Schoenberg, M., 1993. Elastic waves through a simulated fractured medium. Geophysics 58, 964–977.

Hudson, J.A., 1981. Wave speeds and attenuation of elastic waves in material containing cracks. Geophys. J. R. Astron. Soc. 64, 133–150.

Hudson, J.A., 1982. Overall properties of a cracked solid. Math. Pro. Camb. Philos. Soc. 88, 371–384.

Kosik, D.W., 1993. Propagation of a non-linear seismic pulse in an anelastic homogeneous medium. Geophysics 58, 949–963.

Liu, E., Crampin, S., Queen, J.H., Rizer, W.D., 1993. Velocity and attenuation anisotropy caused by microcracks and microfractures in a multi-azimuth reverse VSP. Canadian Journal of Exploration Geophysics 29, 177–188.

Queen, J.H., Rizer, W.D., 1990. An integrated study of seismic anisotropy and the natural fracture system at the Conoco Borehole Test Facility, Kay County, Oklahoma. J. Geophys. Res. 9595, 11255–11273.

Schoenberg, M., Douma, J., 1988. Elastic wave propagation in media with parallel fractures and aligned cracks. Geophysical Prospecting 36, 571–590.

Schoenberg, M., Muir, F., 1989. A calculus for finely layered anisotropic media. Geophysics 54, 581–589.

Thomsen, L., 1986. Weak elastic anisotropy. Geophysics 51, 1954–1966.

Yang, D., 1996. Forward simulation and inversion of seismic wave equations in anisotropic media. PhD Dissertation. Institute of Geophysics, Chinese Academy of Sciences.

Zhang, Z., He, Q., Xu, Z., 1993. Absorbing boundary condition for FD modelling in ZD inhomogeneous TIM. Chinese Geophysical Bulletin 36 (4), 519–527.

Zhang, Z., Quan, Y., Chen, X., Harris, J.M., 1996. FBI for field continuity at interior interfaces for waves in heterogeneous media. STP Annual Report, Vol. 7, No. 1. Stanford University, K1-16.

Zhang, Z., Teng, J., Ho, Z., 1998. Azimuthal anisotropy of seismic velocity, attenuation and quality factor in EDA media (in Chinese). Chinese Sciences, in press.